Catal Lett (2009) 128:197–202
DOI 10.1007/s10562-008-9732-x

Synthesis of Conducting Polymer Supported Pd Nanoparticles in Aqueous Medium and Catalytic Activity Towards 4-Nitrophenol Reduction

S. Harish · J. Mathiyarasu · K. L. N. Phani · V. Yegnaraman

Received: 10 July 2008 / Accepted: 14 October 2008 / Published online: 1 November 2008

Abstract We report here the synthesis of palladium (Pd) nanoparticles incorporated poly-(3,4)ethylenedioxythiophene (PEDOT) matrix in aqueous medium and its catalytic performance towards 4-nitrophenol reduction. This simple one-pot synthesis involving a redox reaction between 3,4-ethylenedioxythiophene and palladium chloride ($PdCl_2$) precursor, leads to the formation of Pd nanoparticles supported on particulate PEDOT. Pd nanoparticles of size 1–9 nm were found to distribute uniformly over the PEDOT matrix. Morphology of the Pd–PEDOT nanocomposite was characterized by field emission-scanning electron microscopy and transmission electron microscopy and the crystallographic details obtained using X-ray diffraction. The chemical nature of the PEDOT support matrix was analyzed using Fourier transform-infra red (FT-IR) spectroscopy. The catalytic activity of the composite was demonstrated using a model reaction, i.e., reduction of 4-nitrophenol to 4-aminophenol. The value of the apparent rate constant, ca. 65.8×10^{-3} s^{-1} obtained using UV visible spectroscopy of the reduction of 4-nitrophenol at the Pd–PEDOT nanocomposite is comparable to those reported for other catalytic systems.

Keywords Heterogeneous catalysis · Palladium · PEDOT · 4-Nitrophenol · Reduction · Nanoparticle

S. Harish · J. Mathiyarasu (✉) · K. L. N. Phani · V. Yegnaraman
Electrodics and Electrocatalysis Division, Central Electrochemical Research Institute, Karaikudi 63006, Tamilnadu, India
e-mail: al_mathi@yahoo.com

1 Introduction

Metal nanoparticles continue to generate intense interest in various fundamental and applied areas of chemistry due to their properties distinctly different from their bulk counterparts. They are extremely reactive by virtue of their intrinsic electronic properties and high *surface-to-volume* ratio. It is now well recognized that the particle stability against agglomeration can be achieved by using stabilizers (solution-phase) and porous solid matrices (heterogeneous catalysis), electronically conductive or otherwise. Most commonly used stabilizers and supports are self-assembled monolayers [1], polymers [2], dendrimers [3–5] functional organic polymers [6], etc. These novel materials find applications in the design of sensors [7], catalysts [8] and electrochromic devices [9].

The synthesis of metal nanoparticles involves reduction of the metal precursor, i.e., metal salts by various reducing agents. Facile oxidation of monomers like pyrrole [10], aniline [11, 12] and thiophene [13] in presence of a few metal salts forms the basis for producing nanocomposites of metal nanoparticles contained in a porous conducting polymer matrix, generated by the oxidation of the monomer. Thiophene-class of monomers, for example, 3,4-ethylenedioxythiophene (EDOT) can function as reducing agents leading to the formation of metal-conducting polymer composites. Such polymer-supported metal nanoparticles have been of current interest due to their properties relevant to (micro-) heterogeneous catalysis, particularly for hydrogenation reactions [14, 15]. In the class of nitro-compounds, the reduction of 4-nitrophenol has been a model reaction to demonstrate the catalytic activity of the metal nanoparticles [16]. We recently have shown that stable dispersions of the Au–poly-(3,4)ethylenedioxythiophene (PEDOT)–PSS nanocomposite [13] can

catalyze this reaction with an apparent rate constant of 43.9×10^{-3} s^{-1}. The *premise* of the present investigation is that palladium (Pd), with its catalytic ability to effect hydrogenation reactions [17–19] can be a suitable candidate for carrying out reduction of nitrophenol and hence be of significance to the synthesis of nanocomposites. Interestingly, we found that the salts of Pd can oxidize the thiophene moiety to produce its conducting polymer while also undergoing reduction to Pd nanoparticles, in this process. EDOT functions as a reducing agent since its oxidation potential is sufficient enough to promote the formation of metal (M = Au, Ag, Pt) nanoparticles. These simultaneous processes lead to the formation of metal–polymer nanocomposites that can be obtained as insoluble powders, porous thin films and can be made water-soluble by including a polymeric stabilizer (and dopant for PEDOT) like, for example, sodium polystyrenesulfonate, as different heterogeneous reactions require conditions specific to the environment, i.e., solid or solution-phase.

It may be noted that a strong reducing agent like borohydride needs a metal catalyst to hydrogenate the nitrocompounds [20, 21]. Since Pd itself is a good candidate as a catalyst for hydrogenation reactions, it is of our current interest to generate its nanocomposites with conducting polymers. Such composites can serve as catalysts not only in heterogeneous catalysis but also in electrochemical processes. Recently, Ilieva et al. [22] reported that Cu–Pd modified PEDOT shows a marked electroactivity towards nitrate reduction and the enhancement in the reduction is due to the adsorption of hydrogen by the deposited Pd within the polymer film.

As part of our current efforts in synthesizing and characterizing conducting polymer–metal nanocomposites, Au_{nano}–PEDOT/PSS system [13] was reported from this laboratory. EDOT was used to reduce $HAuCl_4$ in solutions containing sodium polystyrenesulfonate. In the process of reducing $HAuCl_4$, EDOT is oxidized to form a polymer showing characteristics of PEDOT. It exhibited a very high stability in strong salt solutions, pH-sensitivity and catalytic activity to the reduction of *p*-nitrophenol. In a similar vein, considering the hydrogen adsorption/absorption characteristics of Pd metal, we attempted synthesizing the Pd–PEDOT nanocomposites. Interestingly, when $PdCl_2$ is added to EDOT solution, by an instantaneous reaction, Pd nanoparticles are formed along with the PEDOT polymer from the added EDOT monomer. In addition, Pd is exploited as a catalyst in various coupling reactions like Heck coupling [23], Suzuki coupling [24], hydrogenation of allyl alcohols [25], etc.

In the present study, we report the methodology for the synthesis of Pd–PEDOT nanocomposite as solid powders and dispersions, structural characteristics, morphology and catalytic activity for *p*-nitrophenol reduction.

2 Experimental

2.1 Chemicals

3,4-Ethylenedioxythiophene (EDOT) (Aldrich), sodium 4-polystyrenesulfonate (Aldrich), palladium chloride ($PdCl_2$) (Merck), hydrochloric acid (Ranbaxy), 4-nitrophenol (Ranbaxy), and sodium borohydride (Merck) all of analytical grade were used as received. Aqueous solutions were prepared using Milli-Q water of 18 MΩ.

2.2 Methods

Scanning electron microscopy (SEM) measurements were made using Hitachi Field emission-Scanning electron microscopy (FE-SEM) (Model S4700) with an acceleration voltage of 10 kV in normal mode. X-ray diffraction (XRD) patterns were recorded in a PANalytical diffractometer Model PW3040/60 X'pert PRO operating with Cu K_α radiation ($\lambda = 0.15406$ nm) generated at 40 kV and 20 mA. Scans were done at $3° \text{ min}^{-1}$ for 2θ values between 20° and 90°. Transmission electron microscopy (TEM) examination was made by placing a drop of the sample (dispersed in acetone) onto a copper grid coated with carbon film (400 meshes) and kept aside for drying in air for several hours at room temperature. The TEM images were collected from Philips CM200 microscope working at 200 kV. For infrared spectroscopic measurements, a Thermo-Electron Corp., USA, Nexus 670 model Fourier transform-infra red (FT-IR) spectrometer (DTGS detector) was used. UV–vis spectra were collected using Cary 500 spectrophotometer. The catalytic reduction reaction was carried out in a standard quartz cell of 1 cm path length with about 3 mL volume and spectra were recorded with a time interval of 60 s in a scanning wavelength range of 200–600 nm at 25 °C.

2.3 Synthesis of Pd–PEDOT/Pd–PEDOT–PSS

Synthesis of the Pd-incorporated PEDOT composite involves addition of 1 mL of $PdCl_2$ (5×10^{-3} M) to 10 mL of EDOT (1×10^{-2} M) in aqueous solution. Within a few minutes, the color of the solution changes to black and then slowly black particles are precipitated out from the solution. This observation pertains to the formation of Pd nanoparticles.

As mentioned earlier, EDOT functions as a reducing agent for the synthesis of Pd nanoparticles since its oxidation potential is sufficient enough to drive the reduction of Pd^{2+} while also undergoing oxidation to PEDOT. The PEDOT formed is insoluble in aqueous medium and hence is precipitated. The precipitate was thoroughly washed several times with Milli-Q water and acetone and dried

under vacuum. The dried sample is characterized by XRD, TEM, FT-IR and FE-SEM.

The synthesis of Pd–PEDOT–PSS aqueous dispersion involves the reduction of $PdCl_2$ using EDOT in presence of poly-4-styrene sulfonate sodium (Na–PSS). In brief, 10 mL of EDOT (1×10^{-2} M) was dissolved in water along with 1%Na–PSS (under continuous stirring) which also increases the solubility of EDOT due to the formation of a pseudo-complex [26]. Subsequently, 1 mL of aqueous $PdCl_2$ (5×10^{-3} M) was added slowly to the initial solution under stirring. Color changes instantaneously from colorless to black, indicating the formation of Pd nanoparticles, whereas the precipitation is avoided by the presence of PSS stabilizer.

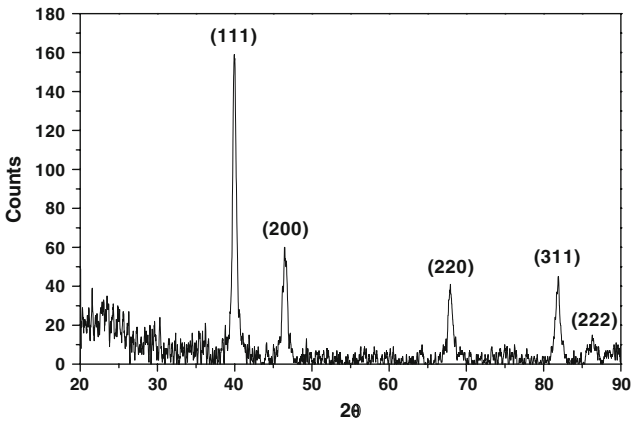

Fig. 2 XRD diffraction pattern of Pd–PEDOT composite

3 Results and Discussion

3.1 Characterization of Pd–PEDOT

Figure 1 shows the FE-SEM image of Pd incorporated PEDOT composite. The image shows that particles are uniformly distributed throughout the porous structure of PEDOT and appears as globules of average size of approx. 80 nm. Since FE-SEM imaging does not distinguish between Pd and PEDOT, XRD analysis was carried out to confirm the presence of Pd in the composite.

XRD analysis of the Pd–PEDOT composite (Fig. 2) shows the reflections at 39.92°, 46.54°, 67.90°, 81.84° and 86.54°, and these peaks correspond to (111), (200), (220), (311), and (222) lattice planes of Pd. Planes were assigned by comparing with the standard Pd and these planes correspond to the *fcc* crystal lattice structure of Pd. No peaks corresponding to PEDOT were observed. The crystallite size of Pd particles was evaluated using Scherrer equation for the (220) peak and is found to be approx. 24 nm in size.

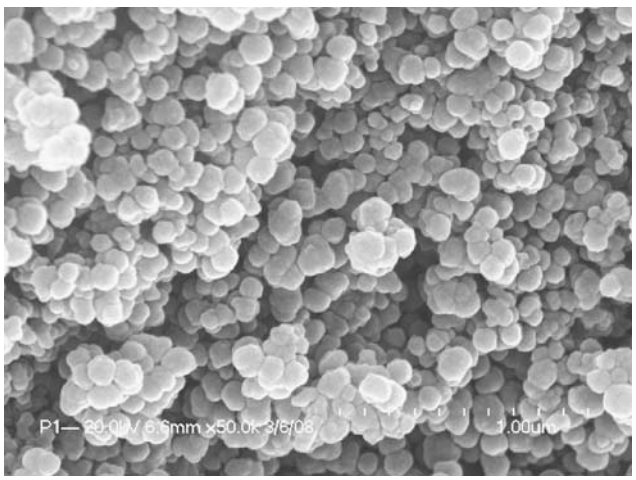

Fig. 1 FE-SEM image of Pd–PEDOT (scale bar 1.00 μm)

The size of the Pd nanoparticles determined using TEM analysis is more reliable than that determined by using Scherrer formula in XRD analysis. FE-SEM gives the size of the globules consisting of a composite of Pd particles and PEDOT, whereas, TEM clearly shows the distinction between the PEDOT matrix and Pd nanoparticles. Figure 3 shows the TEM images of the Pd–PEDOT composite where the black spots correspond to Pd nanoparticles embedded in the polymer matrix. The particles are dispersed uniformly on the polymer matrix and size appears to be ranging from 1 to 9 nm.

The FT-IR spectra of EDOT and Pd–PEDOT in Fig. 4 show that EDOT is completely oxidized by Pd^{2+} to a polymer PEDOT and in turn Pd^{2+} undergoes reduction to Pd^0. The peaks at 1186 and 892 cm^{-1} (EDOT) correspond to =C–H in-plane and out-of-plane deformation vibrations, respectively. Those peaks (marked*) are not present in the spectrum of Pd–PEDOT. A broad peak at 1432 cm^{-1} is attributed to aromatic C=C stretching. These results prove that PEDOT is in the oxidized form with α–α′ coupling. The other peak at 1352 cm^{-1} is due to C–C and C=C stretching of quinoidal structure originating from the thiophene ring. The peaks at 907 and 673 cm^{-1} are assigned to stretching of C–S bond in the thiophene ring and the peaks at 1243 and 1057 cm^{-1} are due to the –C–O–C-bond [27, 28].

3.2 Catalytic Reduction of 4-Nitrophenol

As Pd is known to be an excellent catalyst for hydrogenation reactions, Pd_{nano}–PEDOT can be considered for the reduction of 4-nitrophenol to 4-aminophenol using borohydride. In order to perform this reaction, the use of a water-dispersible catalyst is necessitated. For this, Pd nanocomposite was synthesized using sodium polystyrenesulfonate (Na–PSS) as solubilizer and stabilizer. In addition, Na–PSS also serves as a good dopant in the

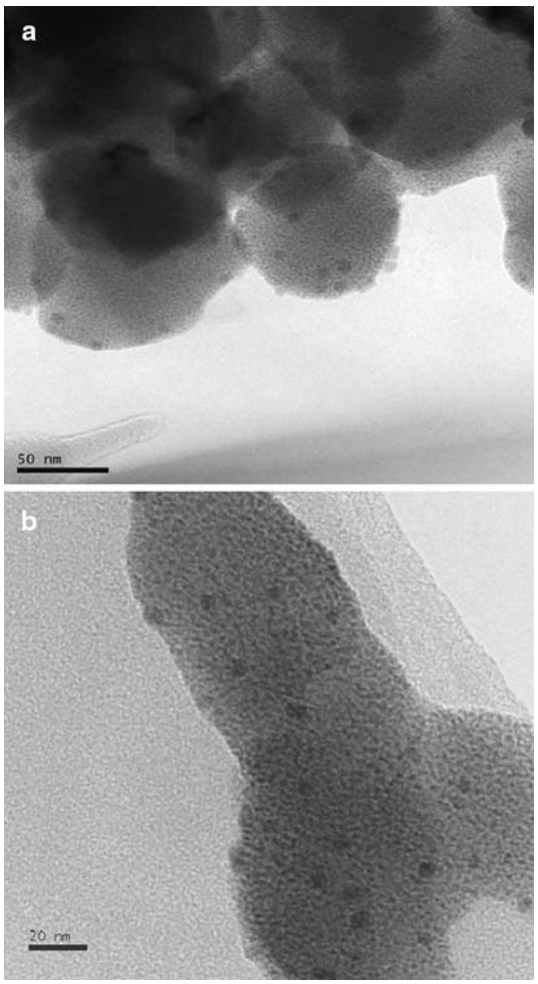

Fig. 3 TEM images of Pd–PEDOT composite (**a**, **b**) and histogram of the particle distribution (**c**)

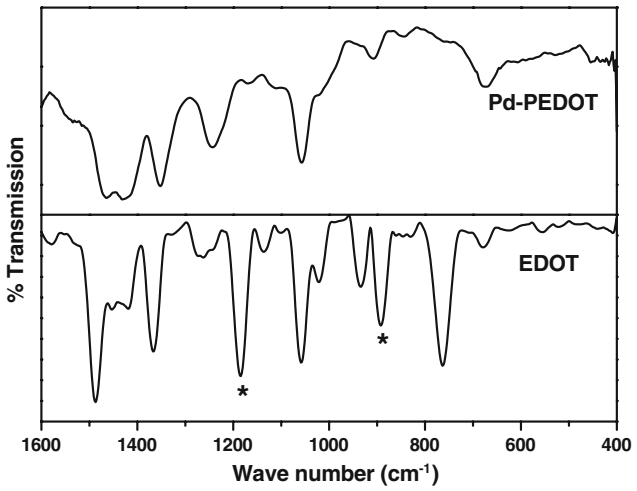

Fig. 4 FT-IR pattern of Pd–PEDOT composite

oxidative polymerization of EDOT and for PEDOT. A porous nanocomposite in the form of metal nanoparticles in the core and the matrix PEDOT being the shell was initially inferred in our earlier work [13]. In the present case, Pd–PEDOT–PSS aqueous dispersion was synthesized by chemically reducing $PdCl_2$ using EDOT as the reductant in presence of Na–PSS which effectively stabilizes the oxidized form of PEDOT compared to other stabilizers during the oxidative polymerization of EDOT [13].

The catalytic application of Pd–PEDOT–PSS nanocomposite is demonstrated by 4-nitrophenol reduction. Initially, the reduction of 4-nitrophenol was demonstrated by several groups using sodium borohydride with a metal catalyst and observed that without a catalyst, sodium borohydride is not an effective reducing agent. In this present work, it is observed that the presence of Pd_{nano}–PEDOT–PSS in aliquot amounts is sufficient for the promotion of nitrophenol reduction with a high value of the apparent rate constant.

Absorption of 4-nitrophenol (1×10^{-6} M) occurs at 313 nm and after the addition of $NaBH_4$, the absorption peak undergoes red shift to 400 nm with a color change from light yellow to dark yellow (corresponding to the generation of nitrophenolate anion) [29]. The absorption peak at 400 nm remains unaltered even after the addition of excess of $NaBH_4$. It confirms that reduction is not achievable in the presence of $NaBH_4$ alone. Interestingly, after the addition of Pd–PEDOT–PSS dispersion (Pd loading: 2 μg/μl) to the initial solution, there was a continuous fading of color leading to discoloration of the solution. In order to follow the kinetics of the reduction reaction, the change in the intensity of absorption of nitrophenolate was monitored using UV–visible spectrophotometry at regular time intervals.

UV–vis spectral studies reveal that (Fig. 5), the only peak due to the nitro group in the presence of $NaBH_4$ at 400 nm corresponds to the formation of nitrophenolate

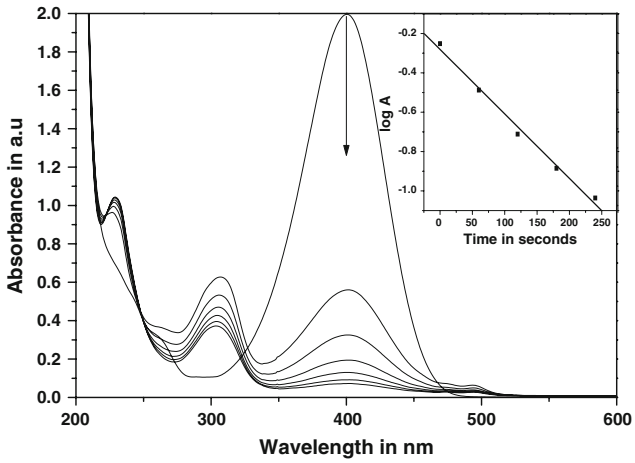

Fig. 5 UV–visible spectrum of 4-nitrophenol reduction in the presence of excess $NaBH_4$ and 40 μl of catalyst (loading: 2 μg/μl) taken at regular intervals; inset: plot between log A vs. time in seconds for the disappearance of 4-nitrophenol absorption at 400 nm

Table 1 Comparison of apparent rate constants for 4-nitrophenol reduction at Pd–PEDOT–PSS with different reported catalyst systems

Composition	Apparent rate constant (s^{-1})	Reference
PNIPA gels (Ag)	3.50×10^{-3}	[30]
β-D-glucose network (Au)	6.54×10^{-3}	[31]
PPI–Dendrimers (Au)	13.2×10^{-3}	[32]
PAMAM–Dendrimers (Au)	3.70×10^{-3}	
Pure Pt	0.12×10^{-3}	[33]
Raney Ni	0.15×10^{-3}	
Ni–Pt (64:36)	0.48×10^{-3}	
Ni–Pt (80:20)	0.90×10^{-3}	
Ni–Pt (96:4)	1.93×10^{-3}	
FGME–Cu	9.00×10^{-3}	[34]
FGME–Ag	9.50×10^{-3}	
FGME–Au	17.5×10^{-3}	
Au_{nano}–PEDOT/PSS^-	43.9×10^{-3}	[13]
Pd_{nano}–PEDOT/PSS^-	65.8×10^{-3}	This work
Microgel-Pd	1.50×10^{-3}	[35]
SPB–Pd	4.41×10^{-3}	
PAMAM–Pd	3.59×10^{-3}	[36]
PPI–Pd	407×10^{-3}	

anion. By adding aliquot amounts (40 µl) of Pd–PEDOT–PSS to the initial solution, there is a concomitant emergence of a peak at 310 and 230 nm that corresponds to the formation of 4-aminophenol. Continuous reduction in the intensity of the peak at 400 nm shows the consumption of 4-nitrophenol. However, there is no proportional increase in the aminophenol peak intensity; probably due to the difference in the molar extinction co-efficient of 4-nitrophenol and 4-aminophenol. In addition, the plot between the logarithmic value of absorbance and time is found to be linear (Fig. 5 inset). The apparent rate constant is calculated from the falling of the peak intensity of 4-nitrophenol at 400 nm and is found to be 65.8×10^{-3} s^{-1}. The apparent rate constant obtained for 4-nitrophenol reduction are rather high in comparison to almost all previous findings in the literature including those obtained with Pd (Table 1).

In our previous report [13], we reported that PEDOT–PSS dispersion alone cannot reduce 4-nitrophenol. Hence, it can be concluded that the reduction takes place only due to Pd nanoparticles. The reaction mechanism can be reasoned by the inherent hydrogen adsorption/desorption characteristics of Pd [19, 20]. Here, the Pd nanoparticles shuttle the hydrogen transport between the $NaBH_4$ and 4-nitrophenol. The shuttling behavior can be reasoned that the Pd nanoparticle adsorbs hydrogen from the $NaBH_4$ and efficiently releases during the reduction reaction (Scheme 1) and hence Pd acts as a *hydrogen carrier* in this reduction reaction.

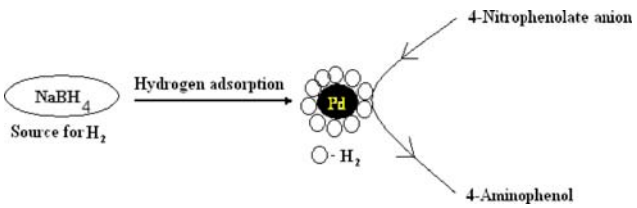

Scheme 1 Schematic representation of the conversion of 4-nitrophenol to 4-aminophenol in the presence of $NaBH_4$ and Pd–PEDOT–PSS

4 Conclusions

A new route for the synthesis of Pd nanopartilces in an aqueous medium at room temperature involving one step and one-pot process is reported. The nanocomposite was characterized using FE-SEM, XRD, TEM and FT-IR. Pd nanoparticles were found to be in *fcc* phase and the particle size was found to be 1–9 nm range from TEM measurements. Catalytic activity of Pd nanoparticles was exploited in the case of 4-nitrophenol reduction. Controlled reaction kinetics allows for calculating the apparent rate constant of the reaction and the value is comparable to the reported ones.

Acknowledgments S. H. thanks to CSIR, New Delhi for the award of Research Internship. The authors thank Dr. A. S. Prakash, CECRI for help in TEM measurements and N. Alagirisamy of Hindustan Unilever Ltd., Bangalore for FE-SEM measurements.

References

1. Ulman A (1996) Chem Rev 96:1533
2. Cole DH, Shull KR, Baldo P, Rehn L (1999) Macromolecules 32:771
3. Wang R, Yang J, Zheng Z, Carducci MD, Jiao J, Seraphin S (2001) Angew Chem Int Ed 40:549
4. Zheng J, Stevenson MS, Hikida RS, Van Patten PG (2002) J Phys Chem B 106:1252
5. Oh SK, Niu Y, Crooks RM (2005) Langmuir 21:10209
6. Králik M, Biffis A (2001) J Mol Catal A Chem 177:113
7. Huang XJ, Choi YK (2007) Sens Act B 122:659
8. Astruc D, Lu F, Aranzaes JR (2005) Angew Chem Int Ed 44:7852
9. Namboothiry MAG, Zimmerman T, Coldren FM, Liu J, Kim K, Carroll DL (2007) Synth Met 157:580
10. Park JE, Atobe M, Fuchigami T (2005) Electrochim Acta 51:849
11. Tseng RJ, Huang J, Ouyang J, Kaner RB, Yang Y (2005) Nano Lett 5:1077
12. Li W, Jia QX, Wang HL (2006) Polymer 47:23
13. Kumar SS, Sivakumar C, Mathiyarasu J, Phani KLN (2007) Langmuir 23:3401
14. Drelinkiewicza A, Waksmundzka A, Makowski W, Sobczak JW, Krol A, Zieba A (2004) Catal Lett 94:143
15. Gelder Elaine A, David Jackson S, Martin Lok C (2002) Catal Lett 84:205
16. Kuroda K, Ishida T, Haruta M (2008) J Mol Catal A: Chem. doi: 10.1016/j.molcata.2008.09.009
17. Yamauchi M, Ikeda R, Kitagawa H, Takata M (2008) J Phys Chem C 112:3294

18. Yoswathananont N, Nitta K, Nishiuchi Y, Satogive M (2005) Chem Commun 40–42
19. Kishorea S, Nelsonb JA, Adairb JH, Eklund PC (2005) J Alloys Compd 389:234
20. Corma A, Serna P (2006) Science 313:332
21. Blaser HU (2006) Science 313:312
22. Ilieva M, Tsakova V, Erfurth W (2006) Electrochim Acta 52:816
23. Karimi B, Enders D (2006) Org Lett 8:1237
24. Klingensmith LM, Leadbeater NE (2003) Tetrahedron Lett 44:765
25. Wilson OM, Knecht MR, Garcia-Martinez JC, Crooks RM (2006) J Am Chem Soc 128:4510
26. Sakmeche N, Aeiyach S, Aaron JJ, Jouini M, Lacroix JC, Lacaze PC (1999) Langmuir 15:2566
27. Li X, Li Y, Tan Y, Yang C, Li Y (2004) J Phys Chem B 108:5192
28. Kvarnström C, Neugebauer H, Blomquist S, Ahonen HJ, Kankare J, Ivaska A (1999) Electrochim Acta 44:2739
29. Panigrahi S, Basu S, Praharaj S, Pande S, Jana S, Pal A, Ghosh SK, Pal T (2007) J Phys Chem C 111:4596
30. Lu Y, Mei Y, Drechsler M, Ballauff M (2006) Angew Chem Int Ed 45:813
31. Liu J, Qin G, Raveendran P, Ikushima Y (2006) Chem Eur J 12:2131
32. Hayakawa K, Yoshimura T, Esumi K (2003) Langmuir 19:5517
33. Ghosh SK, Mandal M, Kundu S, Nath S, Pal T (2004) Appl Catal A: Gen 268:61
34. Pradhan N, Pal A, Pal T (2001) Langmuir 17:1800
35. Mei Y, Lu Y, Polzer F, Ballauff M (2007) Chem Mater 19:1062
36. Esumi K, Isono R, Yoshimura T (2004) Langmuir 20:237